

Supporting Information

Enzyme-controlled reversible generation of coacervate droplets

Karina K. Nakashima^a, Jochem F. Baaij^a and Evan Spruijt^{*a}

a. Institute for Molecules and Materials, Radboud University, Heyendaalseweg 135,
6525 AJ Nijmegen, the Netherlands.

* Correspondence: e.spruijt@science.ru.nl

Supplementary figures

Operational window for differential ADP/ATP coacervation. To evaluate the effect of adding a charged substrate such as PEP to our system, the NaCl titrations were repeated in the presence of 5, 10 and 15 mM PEP. Because the substrate also significantly acidifies the medium, buffer concentration was increased from 50 to 100 mM. Even in a higher ionic strength and with the addition of PEP, there is still a wide operational window where ATP, but not ADP, coacervates with pLys (Fig.S1). Based on these results, a composition of 5 mM ADP or ATP, 100 mM HEPES and addition of 1 equiv. of substrate (e.g., PEP) was considered to be safe in terms of differential coacervation of ADP and ATP.

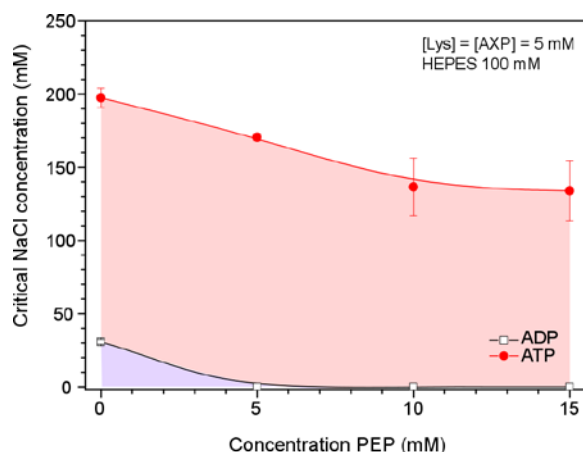


Figure S1: (a) Critical salt concentration for ADP and ATP coacervates with pLys, as determined from turbidity-based titrations. The red shaded region below the red closed circles corresponds to conditions where ATP, but not ADP, coacervates with pLys and is shifted towards lower added NaCl concentrations in comparison to mixtures without PEP and in a weaker buffer.

Coalescence of ATP/pLys coacervate droplets. It is inevitable that the coacervate droplets in our system coalesce, causing the turbidity to decrease slowly in time, even in the absence of an enzymatic reaction that consumes ATP. In order to show that coalescence is indeed a likely cause for the decay observed in e.g. Fig. 4a and 5a, we conducted a control experiment where ATP/pLys coacervates were prepared in the same conditions, and in the presence of PyK and HK, but no substrate was added (Fig.S2). The decrease in turbidity is similar to the decrease observed in other mixtures after reaching the maximum.

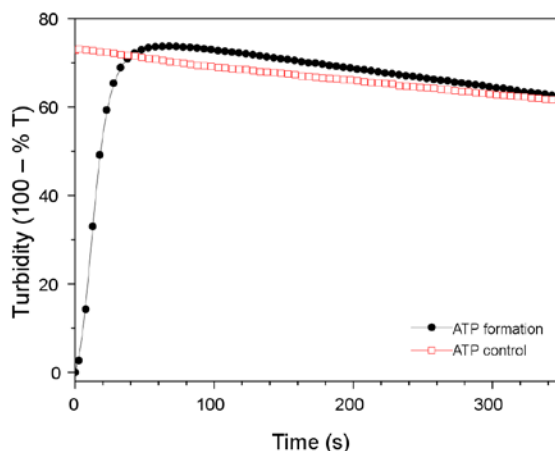


Figure S2: Turbidity decay caused by ATP droplets coalescence. The black curve represents the same dataset from Fig. 4a (formation of ATP catalysed by 1.5 units of PyK upon addition of PEP at $t = 0$). After reaching a maximum turbidity, the decay matches the trend observed for the red curve, which refers to an ATP control without any enzymatic reaction.

Time control over coacervation. In addition to substrate and enzyme ratio, total enzyme concentration also allows us to tune droplet formation. In a system containing initially ADP and a fixed amount of glucose (ratio glucose/PEP = 1/3), the concentrations of PyK and HK were varied together, causing a shift in the time at which ATP/pLys droplets start to assemble.

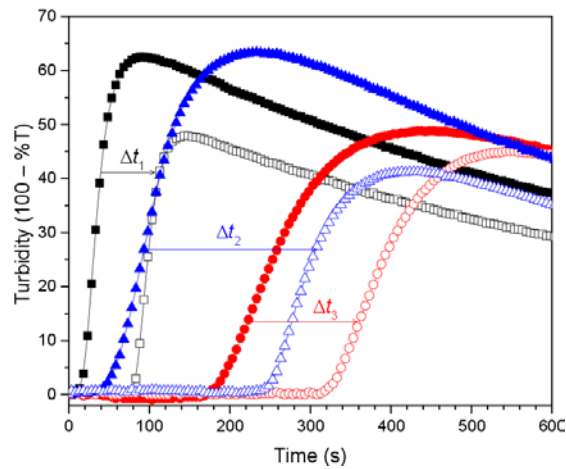
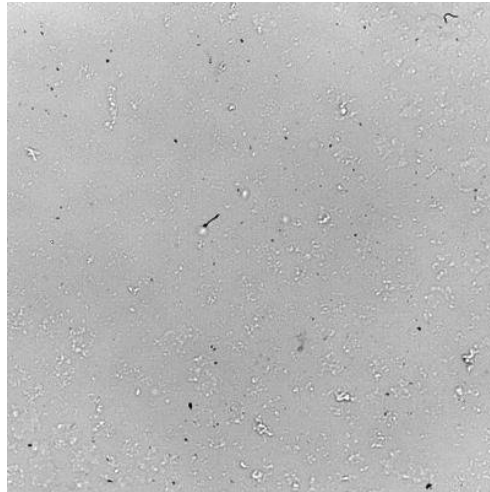


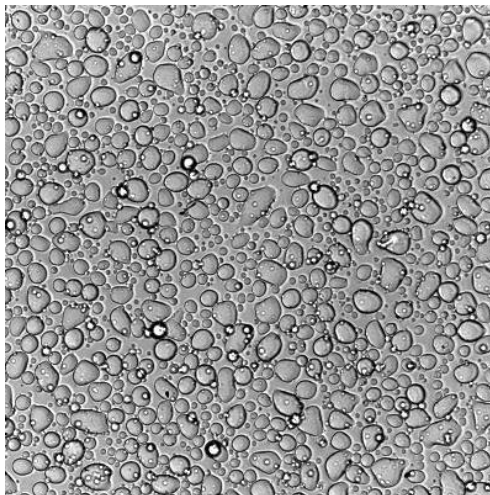
Figure S3: Latent coacervation in a system containing 5 mM ADP and 2.5 mM glucose, to which 7.5 mM of PEP was added at $t = 0$. The ratio between PyK and HK units was held constant at 1:1, but the absolute amount was varied: 1 unit of each (open black squares), 0.5 unit (open blue triangles) and 0.2 unit (open red circles). The closed data points refer to the reference mixtures that did not contain any glucose and received 5 mM of glucose.

Supplementary movies

Enzyme-catalysed condensation and dissolution of ATP/pLys coacervate droplets. We followed the condensation and dissolution of ATP/pLys coacervate droplets shown in Fig. 4a and b by optical microscopy.



Movie 1: Pyruvate kinase-catalysed condensation of ATP/pLys coacervate droplets in the presence of 1 equivalent of PEP observed by bright field optical microscopy. The starting mixture contained 50 mM HEPES, 5 mM MgCl₂, 30 mM NaCl, 5 mM pLys, 5 mM ADP, and 1 unit of pyruvate kinase. At the start of the movie 1 equivalent of PEP was added. Field of view: 275 x 275 μm², total duration: 840 s, speed: 40x real-time.



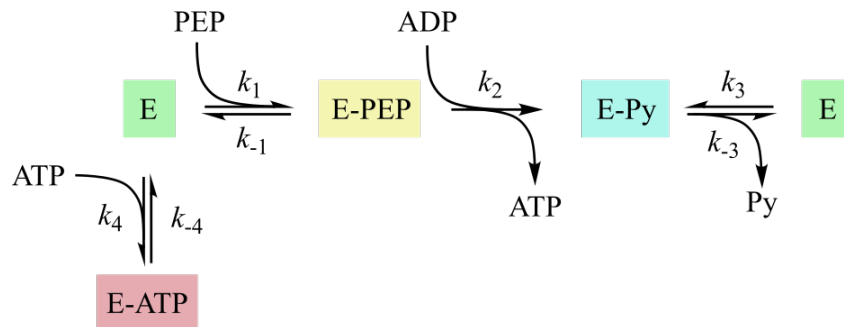
Movie 2: Hexokinase-catalysed dissolution of ATP/pLys coacervate droplets in the presence of 1 equivalent of glucose observed by bright field optical microscopy. The starting mixture contained 50 mM HEPES, 5 mM MgCl₂, 30 mM NaCl, 3 mM pLys, 3 mM ATP, and 0.5 unit of hexokinase. At the start of the movie 1 equivalent of glucose was added. Field of view: 275 x 275 μm², total duration: 870 s, speed: 40x real-time.

Supplementary model data

Kinetic model of enzyme-catalysed coacervate formation and dissolution.

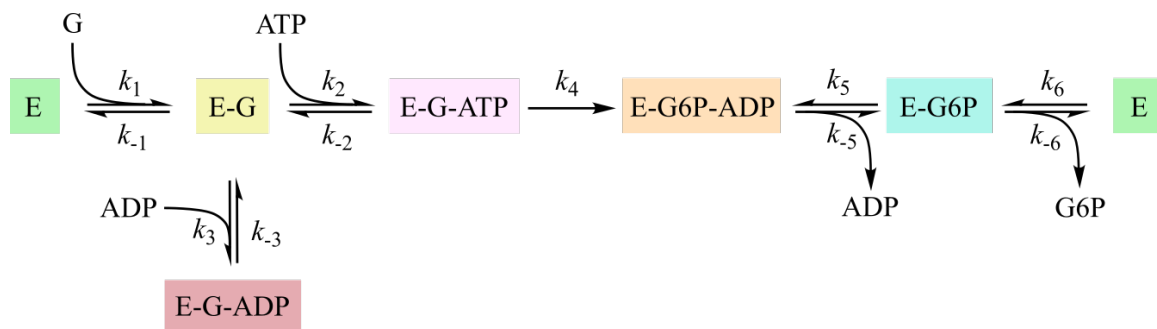
We modelled the reaction network depicted in Fig. 1 as a set of ordinary differential equations (ODE's), which are derived from the underlying reaction mechanisms, similar to the approach taken in the work of Semenov et al [1]. These ODE's were implemented in MATLAB and solved numerically.

In the case of pyruvate kinase-catalysed droplet formation we assumed the following mechanism for the enzyme [2].



where E represents pyruvate kinase, PEP is phosphoenolpyruvate and Py is pyruvate. Note that the product ATP is a reversible inhibitor for pyruvate kinase, by binding to both the enzyme and the enzyme-pyruvate complex. ADP and ATP are thought to bind to the enzyme as a complex with Mg^{2+} . The enzyme concentration corresponding to 1 unit/100 μL was set to 2.2 μM . Finally, based on luciferase assays, we assumed that the ADP was contaminated with 10% ATP.

In the case of hexokinase-catalysed droplet dissolution we assumed the following mechanism for the enzyme [3].



where E represents hexokinase, G is D-glucose and G6P is glucose-6-phosphate. Note that the product ADP is a reversible inhibitor for hexokinase, by binding to both the enzyme-glucose and the enzyme-glucose-6-phosphate complex. ADP and ATP are thought to bind to the enzyme as a complex with Mg^{2+} . The enzyme concentration corresponding to 1 unit/100 μL was set to 3.5 μM .

In both cases, we assumed that reactions only take place in the solution phase, and that ATP is exchanged rapidly between the droplets and the solution. The solution is saturated with ATP at the binodal point [4], which can be estimated from Fig. 2b to be $[ATP]_b = 1.3$ mM. Excess ATP is condensed into droplets by nucleation and growth: $[ATP]_c = [ATP]_i - [ATP]_b$, where $[ATP]_i$ represents the ATP concentration that would be present if phase separation was suppressed, which is the total amount of ATP divided by the total volume. The turbidity was assumed to be directly proportional to $[ATP]_c$. To account for the observed slow coalescence and sedimentation (Fig. S2), we included an empirical linear decrease of turbidity with time, starting from the point of the first droplet condensation.

The individual rates we used to produce the theoretical curves shown in Fig. 4a and b are summarized in Table S1 below.

Table S1: Kinetic constants used for theoretical predictions of pyruvate kinase and hexokinase catalysed droplet formation and dissolution in Fig. 4a and b.

<i>Rate constant</i>	<i>Value</i>
Pyruvate kinase	
k_1	$1.0 \times 10^4 \text{ mM}^{-1} \text{ s}^{-1}$
k_{-1}	$1.0 \times 10^2 \text{ s}^{-1}$
k_2	25 s^{-1}
k_3	$1.0 \times 10^2 \text{ mM}^{-1} \text{ s}^{-1}$
k_{-3}	$1.0 \times 10^2 \text{ s}^{-1}$
k_4	$2.0 \times 10^3 \text{ mM}^{-1} \text{ s}^{-1}$
k_{-4}	$4.0 \times 10^1 \text{ s}^{-1}$
Hexokinase	
k_1	$3.7 \times 10^3 \text{ mM}^{-1} \text{ s}^{-1}$
k_{-1}	$1.5 \times 10^3 \text{ s}^{-1}$
k_2	$4.0 \times 10^3 \text{ mM}^{-1} \text{ s}^{-1}$
k_{-2}	$6.5 \times 10^2 \text{ s}^{-1}$
k_3	$5.0 \times 10^3 \text{ mM}^{-1} \text{ s}^{-1}$
k_{-3}	$2.0 \times 10^4 \text{ s}^{-1}$
k_4	15 s^{-1}
k_5	$2.0 \times 10^3 \text{ mM}^{-1} \text{ s}^{-1}$
k_{-5}	$2.0 \times 10^3 \text{ s}^{-1}$
k_6	$1.2 \times 10^2 \text{ mM}^{-1} \text{ s}^{-1}$
k_{-6}	$1.5 \times 10^3 \text{ s}^{-1}$

References

- [1] S. N. Semenov, A. S. Y. Wong, R. M. van der Made, S. G. J. Postma, J. Groen, H. W. H. van Roekel, T. F. A. de Greef and W. T. S. Huck, *Nature Chem.*, 2015, **7**, 160.
- [2] C. Wang, L. R. Chiarelli, P. Bianchi, D. J. Abraham, A. Galizzi, A. Mattevi, A. Zanella and G. Valentini, *Blood*, 2001, **98**, 3113.
- [3] G. Noat, J. Ricard, M. Borel and C. Got, *Eur. J. Biochem.*, 1968, **5**, 55.
- [4] E. Spruijt, A. H. Westphal, J. W. Borst, M. A. Cohen Stuart and J. van der Gucht, *Macromolecules*, 2010, **43**, 6476.